A BAYESIAN APPROACH TO SPACEBORN HYPERSPECTRAL OPTICAL FLOW ESTIMATION ON DUST AEROSOLS

Fabian E. Bachl, Christoph S. Garbe

University of Heidelberg
Interdisciplinary Center for Scientific Computing
Heidelberg, Germany

Paul Fieguth

University of Waterloo
Dept. of Systems Design Engineering
Waterloo, Ontario, Canada

ABSTRACT

The significant role dust aerosols play in the earth's climate system and microbial nutrition cycles have lead to increased efforts of employing remote sensing to monitor their genesis, transport and deposition. This contribution extends earlier approaches of using Bayesian hierarchical models to extract dust activity from multispectral MSG-SEVIRI measurements by focusing on the signal-to-noise ratio with respect to post hoc motion analysis via optical flow. While interpreting also the latter in a completely Bayesian fashion, we show that our novel dust indication scheme reduces background noise and thereby renders the optical flow more decisive in terms of detecting even faint dust plumes. As a side effect of the indicators stability in case of dust absence, we point out the potential usage of its temporal variance to characterize dust at an early stage of the genesis and thus close to the corresponding source region.

Index Terms— Bayesian methods, Multispectral imaging, Aerosols, Image motion analysis, Image segmentation

1. INTRODUCTION

Dust aerosol has a significant impact on the atmospheric radiation budget by influencing microphysical cloud processes, scattering and absorbing shortwave radiation and absorbing and re-emitting longwave radiation [1]. Its effect on the global climate system is additionally underlined by its global depositions that provides mineral nutrients to oceanic and terrestrial ecosystems which ultimately influence the CO_2-cycle [2].

Satellite remote sensing is a powerful instrument for assessing atmospheric dust distribution. In particular the Meteosat Second Generation (MSG) Spinning Enhanced Visible and InfraRed Imager (SEVIRI) is well suited for this task. Using differences of its 8.7 μm, 10.8 μm and 12.0 μm infrared Brightness temperature (BT) measurements, the instrument is capable of capturing sub-daily processes like short-termed cycles of dust emission at intervals of 15-minutes and a resolution of 3x3 km at nadir [3].

As shown by Bachl et al. [4], a Bayesian Hierarchical Model (BHM) can be employed to generate a linear predictor (LP) from SEVIRI data that serves as an indicator for the presence of dust and facilitates determining the trajectory of dust plumes via optical flow. Using the resulting flow field to warp back the thresholded LP can then serve to point out spatial regions that are likely to be the source of the plume (left columns of Figure 1). However, since the LP is a background dependent linear mixture of infrared channels, it also carries over the noise incorporated by the signal. This results in two interwoven problems. On the one hand, as shown in Figure 1(b) and (d), faint dust is easily underestimated by the LP but lowering the detection threshold is likely to induce false positives which then interfere with the source detection. On the other hand, as shown in Figure 1(f), especially in cases of faint dust the movement as represented by the optical flow is a strong indicator for its presence.

In this contribution we extend previous approaches in the sense that the LP is not a linear projection but a probabilistic mapping of the signal. We show that this increases the temporal signal-to-noise ratio of the LP forward differences, a quantity that enters the optical flow but also appears to be a promising indicator for dust source detection. Additionally, our method also yields a higher expressiveness of the corresponding optical flow compared to flow based on multiple channels or a projection according to Linear Discriminant Analysis.

2. METHODS

We begin this section with an introduction into the class of models we are employing as well as the type of inference we are performing. Thereafter, different dust indication schemes are elucidated and a Bayesian interpretation of optical flow is given.

2.1. Generalized Linear Models

Recent developments in computational statistics, known as Integrated Nested Laplace Approximations (INLA), have paved the way for efficient inference in a subclass of BHMs, the Generalized Linear Model (GLM) [5]. In this class, each variable in the set of observations $\{y_i\}_{i\in 1\dots N}$ is assumed to come from an exponential family distribution parameterized by the inverse image μ_i of a structured additive predictor η_i under a link function $g(\cdot)$, i.e. $g(\mu_i) = \eta_i$. Each η_i is linearly generated by a subset of a possibly very high dimensional latent Gaussian Markov Random Field (GMRF) $\mathbf{x}$ and in most cases μ_i defines the mean of the distribution generating y_i. Using local covariate vectors $\mathbf{z}^{(i)}$ and $\mathbf{u}^{(i)}$ the process generating y_i can be work in two ways. A subset $\{x_k\}_{k\in K}$ of the latent field $\mathbf{x}$ can serve as linear projection coefficients. Another subset $\{x_j\}_{j\in J}$ can represent function evaluations $f^{(j)} := x_j$ at the covariate values $u_j^{(i)}$. Summing up over both sets then results in the following linear predictor:

$$\eta_i = \sum_{j\in J} f^{(j)}(\mathbf{u}_j^{(i)}) + \sum_{k\in K} x_k \mathbf{z}_k^{(i)} \tag{1}$$

The corresponding likelihood functions of y_i as well as the prior distribution of the latent field $\mathbf{x}$ themselves depend on a set $\boldsymbol{\Theta}$ of parameters that again obey predefined prior distribution. The overall

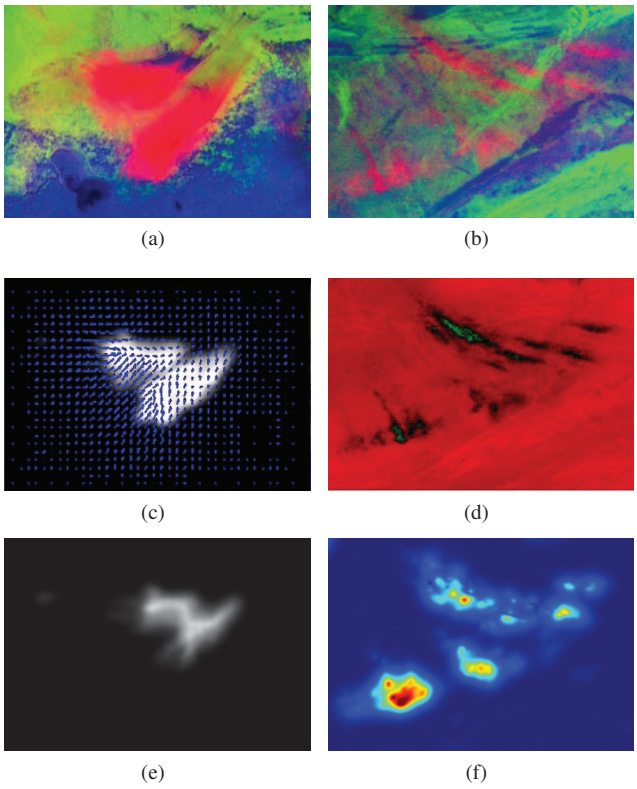

(a) (b) (c) (d) (e) (f)

Fig. 1. In (a) and (c) a dust plume and the corresponding positive part of the LP along with its optical flow field are displayed. Warping back the LP accoring to the corresponding sequence of flow fields results in the source map shown in (e). The dust plumes shown in (b) are rather faint, which leads to low (black) or even negative values (red) of the LP shown in (d). Subfigure (f) shows the normalized magnitude of the corresponding optical flow.

model factorizes into multiple stages and is therefore hierarchically structured:

$$p(\mathbf{x}, \mathbf{\Theta}|\mathbf{y}) \propto p(\mathbf{\Theta})p(\mathbf{x}|\mathbf{\Theta}) \prod_i p(y_i|x_i, \mathbf{\Theta}) \tag{2}$$

Given a model of this kind, the INLA technique yields approximations $\tilde{p}$ to the marginals for both, the latent as well as the parameter posteriors:

$$\tilde{p}(x_i|\mathbf{y}) \approx \int p(x_i|\mathbf{y}, \mathbf{\Theta})p(\mathbf{\Theta}|\mathbf{y})\, \mathrm{d}\mathbf{\Theta} \tag{3}$$

$$\tilde{p}(\Theta_{j\in J}|\mathbf{y}) \approx \int p(\mathbf{\Theta}|\mathbf{y})\, \mathrm{d}\mathbf{\Theta}_{J\setminus\{j\}} \tag{4}$$

2.2. Background Radiance

A crucial part of our classification technique is that it takes an estimate of the background radiation into account, an approximation to the earth's brightness temperature under clear sky conditions. Given a MSG-SEVIRI image sequence $I_{\lambda,t,i}$ for time t, spatial location i we utilize a maximum-intensity criterion to determine this estimate:

$$B_{\lambda,t,i} = \max_{\hat{t}} \sum_{\hat{\lambda}} I^2_{\hat{\lambda},\hat{t},i} \quad \text{s.t.} \quad \hat{t} \in \{t + 96k | k \in \mathcal{N}\} \tag{5}$$

Note that in this equation $\hat{t}$ iterates over identical times over different days since MSG-SEVIRI delivers 96 images per day. This way, for a data set I covering multiple days, a single clear day is sufficient for the estimate if a decrease of the radiation is assumed in case of dust and water clouds covering the background. The background estimation procedure is, however, independent of the detection techniques explained in the following paragraph. It is therefore possible to employ other techniques to determine this estimate, e.g. applying the method introduced by Liu et al. [6] to an extended data set.

2.3. Detection methods

Referring to our novel approach of dust detection as Latent Signal Mapping (LSM), we compare it to the well known method of Linear Discriminant Analysis (LDA). For reasons of completeness we also give the definition of the method recently proposed by Bachl et al. [4] but the respective results are omitted due to their similarity to those of LDA with respect of the analysis at hand. We will refer to this method as Latent Projection Functions (LPF). All three methods can be expressed as BHMs and model the probability of a pixel containing dust activity as a binomial distribution with a mean given by the logisitic sigmoid of the LP, i.e.:

$$p(\text{dust}) = \mathcal{B}(1/(1 + exp(-\eta)) \tag{6}$$

In case of LDA, the LP is a simple linear projection where f_λ and g_λ are the frequency-specific coefficients with Gaussian priors and c is an intercept variable:

$$\eta^{\text{LDA}} = \sum_\lambda f_\lambda \cdot I_\lambda + \sum_\lambda g_\lambda \cdot B_\lambda + c \tag{7}$$

LPF extends LDA with f_λ and g_λ being Continuous Random Walks modeling functions over the background radiation:

$$\eta^{\text{LPF}} = \sum_\lambda f_\lambda(B_\lambda) \cdot I_\lambda + \sum_\lambda g_\lambda(B_\lambda) + c \tag{8}$$

Our new method has a different concept. Here, the input signal is not projected by a background dependent function but enters the now two-dimensional domain of the latent functions f_λ onto which a lattice Random Walk prior is assigned:

$$\eta^{\text{LSM}} = \sum_\lambda f_\lambda(B_\lambda, B_\lambda - I_\lambda) \tag{9}$$

2.4. Optical Flow

In order to perform tracking of the movement of dust in the atmosphere we estimate the optical flow as defined by Horn & Schunck [7]. Even though it is commonly treated in a variational framework of functional minimization, it finds a straight forward probabilistic interpretation. The general idea is expressed by the Brightness Constancy Equation:

$$\exists k\, \forall t \quad \eta(x(t), y(t), t) = k \tag{10}$$

Performing a Taylor expansion on this equation yields, if Gaussian errors are assumed, the likelihood of the horizontal and vertial optical flow fields $\mathbf{u}$ and $\mathbf{v}$ to generate a given temporal sequence of spatial data:

$$\eta_x u + \eta_y v + \eta_t = \epsilon, \quad \epsilon \sim \mathcal{N}(0, \sigma^2) \tag{11}$$

Since this system is underdetermined it is assumed that the flow fields are smooth across space. This is expressed by simultaneously

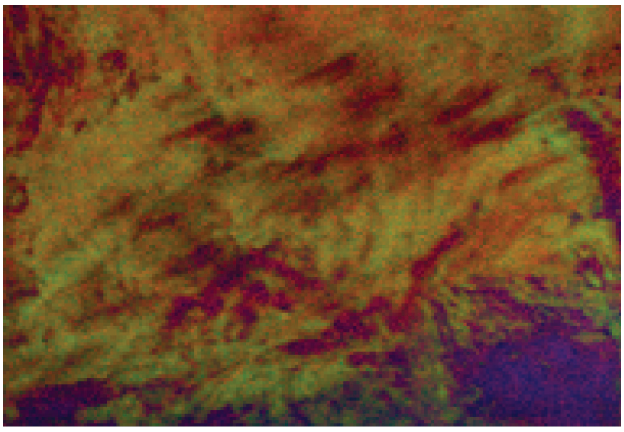

Fig. 2. Multiple faint dust plumes visible as dark to purple areas around the center of the image. The measurement was taken approximately 30 minutes after the beginning of the dust event.

optimizing a penalty term L on the squared Euclidian norm of their gradient integrated over the image domain Ω:

$$L(\alpha) = \int_{\Omega} \alpha^2 (|\nabla \mathbf{u}|^2 + |\nabla \mathbf{v}|^2)\, d\Omega \tag{12}$$

Here, α is a fixed parameter controling the smoothness of the flow fields and is in most cases chosen by application specific empirical work. Discretizing the term is then equivalent to imposing a Gaussian distribution with variance α on the spatial differences of the flow fields, e.g. in case of $\mathbf{u}$:

$$u_i \sim \mathcal{N}(\frac{1}{|N(i)|} \sum_{j \in N(i)} u_j, \alpha^2) \tag{13}$$

In the context of GMRFs this is known as as Conditional Autoregression (CAR) model and can be understood to define a prior distribution over $\mathbf{u}$ and $\mathbf{v}$. Together with the likelihood defined above and additional prior distributions of σ and α this formulation results in a BHM with the following posterior of the optical flow:

$$p(\mathbf{u}, \mathbf{v} | \nabla\eta, \sigma, \alpha) \propto p(\nabla\eta | \mathbf{u}, \mathbf{v}, \sigma) p(\mathbf{u}, \mathbf{v} | \alpha) p(\sigma) p(\alpha) \tag{14}$$

3. EXPERIMENTAL RESULTS

As we are focusing on faint dust, we inspect temporal sequences of two events that are characteristic in that sense. Event A, shown in Figure 1(b), is a five hour sequence of multiple faint plumes with a very smooth trajectory. Event B, shown in Figure 2, is composed of two hours of multiple small plumes coming from comparably close but distinguishable source areas.

3.1. Temporal signal to noise ratio

Figure 3 displays the normalized standard deviations of the temporal forward differences for the falsecolor representation and the linear predictors of LDA and LSM. We omit results for the LPF method since they are very similar to those of LDA. For both events it is obvious that the activity of the LP of LSM is a lot more expressive than for FC and LDA when comparing dusty and dust free regions. Also, in case of event B, for which even visual discrimination between dusty and non-dusty regions is challenging, the forward differences seem to be an appealing feature for the detection of the relatively small dust sources.

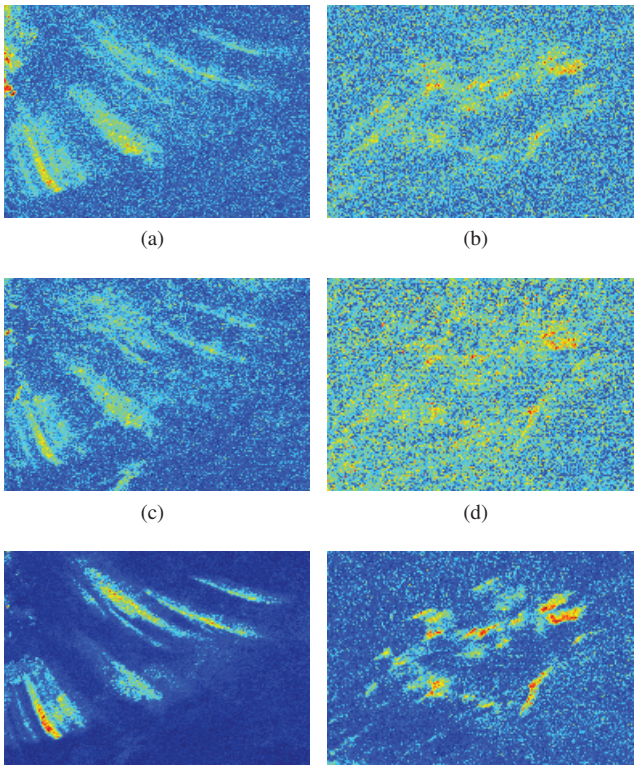

Fig. 3. A comparison of spatially normalized standard deviations calculated from the temporal forward differences of two dust events (left and right column, respectively). Subfigures (a) and (b) refer to the mean deviation of the SEVIRI falsecolor representation, (c) and (d) to the LP of LDA and (e) and (f) to the LSM method.

3.2. Optical Flow

In order to get an idea of how the described noise enters the optical flow, we compare its magnitude standard deviation along the event sequences for the LDA and LSM predictors with optical flow determined jointly from the three channels of the falsecolor representation. As can be seen from Figure 4, a projection according to LDA is not necessarily improving the optical flow with respect to dust activity monitoring. Though LDA seems to improve the signal of the faint plume in the upper region of event A, seemingly dust free regions at the outer regions of both inspected regions reveal flow induced by the background. It should be mentioned that results for the LPF method are again omitted since they suffer from similar problems, even though the mentioned plume induces a slightly better signal than in case of LDA. Contrarily, the magnitude variance of the flow determined from the LSM LP does not seem to suffer from this imbalance. Dusty regions clearly show activity and resemble the appearance of the imagery and forward differences while dust free regions exhibit only slight variations.

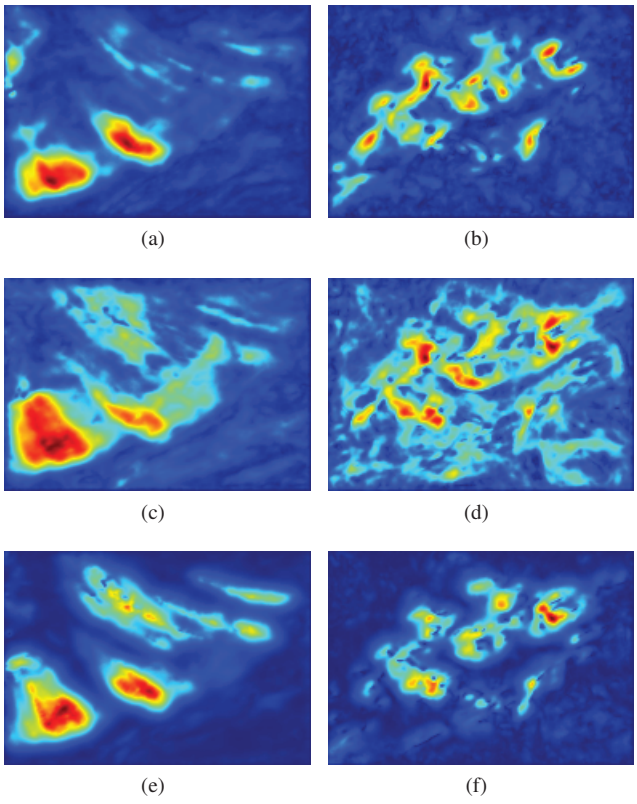

Fig. 4. A comparison of the spatially normalized temporal standard deviation of the flow magnitude of two dust events (left and right column, respectively). Subfigures (a) and (b) refer to the optical flow determined jointlyfrom the SEVIRI falsecolor imagery, (c) and (d), (e) and (f) refer to the flow based on LDA and LSM, respectively.

4. CONCLUSION

Our results show that the proposed method of Latent Signal Mapping is superior to other Bayesian approaches of detecting dust aerosols in multispectral data. In particular the propagation of the signal intrinsic noise to the scalar indicating the presence of dust is strongly reduced. This greatly facilitates contributing the resulting optical flow to dust activity and motivates further integration of this quantity into the detection mechanism. We were also able to point out that the LSM temporal forward differences are comparably expressive in terms of indicating early dust activity. This is a potentially supporting mode in terms of tracing dust back to its source area which is a particulary desirable goal from the perspective of environmental sciences.

5. REFERENCES

[1] I. N. Sokolik, D. M. Winker, G. Bergamenti, D. A. Gillette, G. Carmichael, Y. J. Kaufman, L. Gomes, L. Schuetz, and J. Penner, "Introduction to special section: Outstanding problems in quantifying the radiative impacts of mineral dust," *Journal of Geophysical Research*, vol. 106 (D16), pp. 18015–18027, 2001.

[2] T. D. Jickells, Z. S. An, K. K. Andersen, A. R. Baker, G. Bergametti, N. Brooks, J. J. Cao, P. W. Boyd, R. A. Duce, K. A. Hunter, H. Kawahata, N. Kubilay, J. Laroche, P. S. Liss, N. Mahowald, J. M. Prospero, A. J. Ridgwell, I. Tegen, and R. Torres, "Global iron connections between desert dust, ocean biogeochemistry, and climate," *Science*, vol. 308, pp. 67–71+, 2005.

[3] K. Schepanski, I. Tegen, B. Laurent, B. Heinold, and A. Macke, "A new saharan dust source activation frequency map derived from msg-seviri ir-channels," *Geophysical Research Letters*, vol. 34, pp. 5 PP, 2007.

[4] Fabian E. Bachl and Christoph S. Garbe, "Classifying and tracking dust plumes from passive remote sensing," in *Proceedings of the ESA, SOLAS & EGU Joint Conference "Earth Observation for Ocean-Atmosphere Interaction Science"*, 2012.

[5] Havard Rue, Sara Martino, and Nicolas Chopin, "Approximate bayesian inference for latent gaussian models by using integrated nested laplace approximations," *Journal Of The Royal Statistical Society Series B*, vol. 71, no. 2, pp. 319–392, 2009.

[6] Chenyi Liu, Paul Fieguth, and Christoph S. Garbe, "Background subtraction and dust storm detection," in *Geoscience and Remote Sensing Symposium, 2012. IGARSS 2012, Munich. IEEE International*, 2012.

[7] Berthold K. P. Horn and Brian G. Schunck, "Determining optical flow," *Artificial Intelligence*, vol. 17, no. 1-3, pp. 185–203, 1981.